Investigating the Effect of Intra-Subject Variability in Seismocardiogram Analysis

Eda Demirsoy
Physics
Bogazici University
Istanbul, Turkey
eda.demirsoy@std.bogazici.edu.tr

Beren Semiz
Electrical and Electronics Engineering
Koc University
Istanbul, Turkey
besemiz@ku.edu.tr

***Abstract*—Seismocardiogram (SCG) signal corresponds to the local chest vibrations originating from the contraction of the heart and has been leveraged to assess cardiovascular parameters and pathologies, especially in studies focusing on wearable system design. Two common challenges encountered in the analysis of SCG are the presence of inter-subject and intra-subject variability, affecting the generalizability and performance of the models. In this work, we focus on the intra-subject variability to show how the local body compositions and surrounding systems affect the morphology of the SCG signals. More specifically, we investigated the effects of sensor location and respiration phases on the SCG signals. Analysis of tri-axial SCG signals from 16 different locations on torso was treated as a 16-class classification problem, whereas the effect of inhalation and exhalation was formulated as a binary classification task. Using features from 5 different groups, our models achieved a distinction rate of %92 and %90 for the sensor location and respiration effect, respectively. Additionally, we showed that the effect of intra-subject variability is not the same for different SCG axes or feature groups. Overall, intra-subject variability has a great impact on the SCG characteristics, thus the inaccuracies stemming from sensor location or surrounding physiological systems should be minimized during analyses to have more generalizable models.**

***Index Terms*—seismocardiogram, electrocardiogram, respiration, intra-subject variability, inter-subject variability**

I. Introduction

Physiological signals can provide valuable information regarding the underlying physiological events and potential health-related pathologies. With the advancements in sensor technology, these physiological signals can easily be collected using sensors embedded into electronic devices and wearable systems. One of the most popular signals used in wearable system design is the seismocardiogram (SCG) signal. SCG assesses the heart from mechanical perspective and represents the thoracic oscillations resulting from the rhythmic contractions of the heart and the expulsion of blood from the ventricles into the vascular system [1].

SCG can be measured using a tri-axial accelerometer mounted on mid-sternum, acquiring the vibrations in the dorso-ventral, lateral, and head-to-foot axes. The peaks and valleys on each axis corresponds to specific valve movements in the cardiac cycle, such as aortic opening, mitral closing, etc. In the literature, SCG signal has been leveraged in various applications, such as heart failure detection [2]; systolic time interval, stroke volume and heart failure prediction [3]–[5]; respiration phase extraction [6], [7], and valvular heart disease assessment [8]. Although SCG holds a significant potential to quantify underlying cardiovascular and cardiorespiratory mechanisms, its analysis is often challenging due to artifacts and variability introduced by various factors.

Two common challenges encountered in the analysis of SCG (and numerous other physiological signals) are the presence of inter-subject and intra-subject variability. Inter-subject variability refers to the differences observed in physiological signals across different individuals, stemming from variations in underlying physiology, anatomy, and stressors. While subject-specific models were suggested as an alternative approach, adopting such a method impairs the generalizability of the proposed frameworks [9]. On the other hand, intra-subject variability occurs within the same subject across consecutive recordings, resulting from the differences in sensor location, stress, exercise level, etc. Especially when the utmost aim is to achieve individualized treatment and remote monitoring, the inaccuracies stemming from intra-subject variability should be minimized to have more generalizable and accurate models.

In our previous work, we investigated and quantified the inter-subject variability observed in SCG signals using linear predictive analysis. We showed that the variability in the medium between the accelerometer and heart across different people will result in changing filtering effect on the SCG signals as each person has a unique combination of bone, muscle, fat and skin cells [10]. In this work, contrarily, we focused on the intra-subject variability to show how the local body compositions and surrounding systems affect the morphology of the SCG signals. More specifically, we focused on the effects of sensor location and respiration phases on the SCG signals. In addition, for the first time, we showed which feature groups and SCG axes (directions) are affected the most by the intra-subject variability introduced by the sensor location and respiration activity.

II. METHODS

A. Dataset Description

In this paper, publicly available *Multichannel Seismocardiography: An Imaging Modality for Investigating Heart Vibrations* dataset from the *Mendeley Data* database was used. [11]. All the measurements were performed

using a system of 16 tri-axial accelerometers, a 3-lead electrocardiogram (ECG), and a respiration belt. The X, Y and Z axes of the accelerometer were corresponding to the lateral, head-to-foot and dorso-ventral directions, respectively. The sensor was positioned within a 4x4 grid upon the thoracic region of the subjects in conjunction with a 3-lead ECG setup and a respiration belt, as shown in Figure 1. The study involved the collection of measurements from a cohort comprising 13 male subjects (Age: 27 $\pm$ 4, BMI: 24 kgm^{-2} $\pm$ 4 kgm^{-2}). During data collection, the participants were positioned in a supine posture for 3 minutes. Data was recorded continuously at 500 Hz.

B. Pre-Processing and Signal Segmentation

Initially, the SCG, ECG, and respiration signals underwent filtration using Butterworth band-pass filters. The SCG filters were configured with a second-order and a passband range of 0.05-90 Hz, the ECG filters were set with a fourth-order and a passband of 0.5-35 Hz, and the respiration filters were adjusted to a second-order with a passband of 0.01-1 Hz. Subsequently, a bidirectional application of the filters was implemented to prevent any alteration in the phase of the signals.

After filtering, the SCG and ECG signals were segmented into exhalation and inhalation cycles using the minima and maxima locations on the respiration signal. Segments characterized by a transition from one local minimum to the subsequent closest maximum were categorized as inhale cycles, while segments marked by a transition from one local maximum to the subsequent closest maximum and then to the next closest minimum were denoted as exhale cycles. The exhalation and inhalation segments were stored for each subject for further processing. A representative inhalation-exhalation segmentation is presented in Figure 2.

Following this segmentation process, for every SCG segment labeled with exhalation or inhalation, a single representative SCG beat was generated. This was achieved by identifying R peaks on each ECG segment and using them to identify individual beats on each SCG segment. The duration of each beat was set as the minimum R-R interval. The identified SCG beats induced by inhalation and exhalation were segregated into separate matrices for subsequent analysis. Segments lacking a complete beat were excluded, while segments containing two or more beats only retained the first beat. In total there were 30362 beats from 13 subjects, 16 locations, 3 axes.

C. Feature Extraction

After the segmentation process, 58 features were extracted from each SCG beat, in all three directions. These features can be categorized into the following groups:

1) Time Domain Features: The selected characteristics consist of the initial three minimum and maximum data points, alongside their respective half-lengths and amplitudes within the 0-250 millisecond timeframe. Additionally, the first three minimum and maximum data points, their half-lengths, and amplitudes were considered within the 250-500 millisecond interval. Moreover, parameters such as energy, entropy, and zero crossing rate (ZCR) were derived and analyzed. Energy represents the total energy within the signal and is computed through the summation of the squared amplitudes of the signal's samples. Moreover, entropy serves as a metric for quantifying the abrupt variations in the signal's energy levels. A notable observation is that during instances of sudden signal alterations, a decrease in entropy is anticipated. ZCR characterizes the frequency of changes in polarity within the signal segment. This feature is commonly employed to evaluate the level of noise present in the signal. Broadly, a positive correlation is observed between the level of signal noise and the value of ZCR, suggesting that higher noise levels tend to correspond with elevated ZCR values [12].

2) Frequency Domain Features: Due to their dynamic nature, physiological signals manifest time-varying statistics. The application of wavelet transform enables the analysis of non-stationary signals like SCG signals across various scales, proving advantageous [8]. Consequently, a 1D multilevel discrete wavelet transform was employed using a level-6 sym4 wavelet. The choice of six levels was crucial to adequately decompose the signal, allowing analysis up to the respiration band [7]. Furthermore, the first two consecutive prominent frequencies and spectral rolloff features were extracted. The spectral rolloff, relating to the frequency threshold below which a specific percentage of the signal's energy is concentrated, is a valuable metric in signal analysis. In addition to the aforementioned features, bandpowers were computed at 10 Hz intervals between 0.1-90 Hz resulting in 9 features. Bandpower represents the spectral power within a defined frequency range, holding significance in exploring various wave components. This feature is particularly instrumental in the examination of signals with distinctive spectral characteristics.

3) Fractal Dimension Features: Fractal analysis techniques are utilized to assess the complexity of the SCG signal by measuring its fractal dimension. The key feature of fractal structures is their self-replication across different scales; while not identical, they consistently display statistical properties as the observation scale changes. In the literature, it was shown that there is a clear distinction between the ranges of inter- and intra-subject variation in fractal measurements across the different movements studied [13]. Katz proposed an algorithm for computing the fractal dimension (FD), which reduces computational complexity by determining the distance between two consecutive points for FD calculation. This distance serves as a metric of irregularity in the signal, which is represented as a one-dimensional time series [14]. Thus, Katz's fractal dimension analysis was also included in the feature set.

4) Non-linearity Features: As nonlinear features, the largest Lyapunov exponent and values of SD1 and SD2 from Poincaré plot analysis were extracted. The Poincaré plot is a nonlinear approach for analyzing heart rate variability (HRV), wherein diagrams are utilized to graph inter-beat intervals against preceding inter-beat intervals. SD1 denotes short-term variability in heart rate, whereas SD2 delineates long-term variability. It was found that there are no significant differences

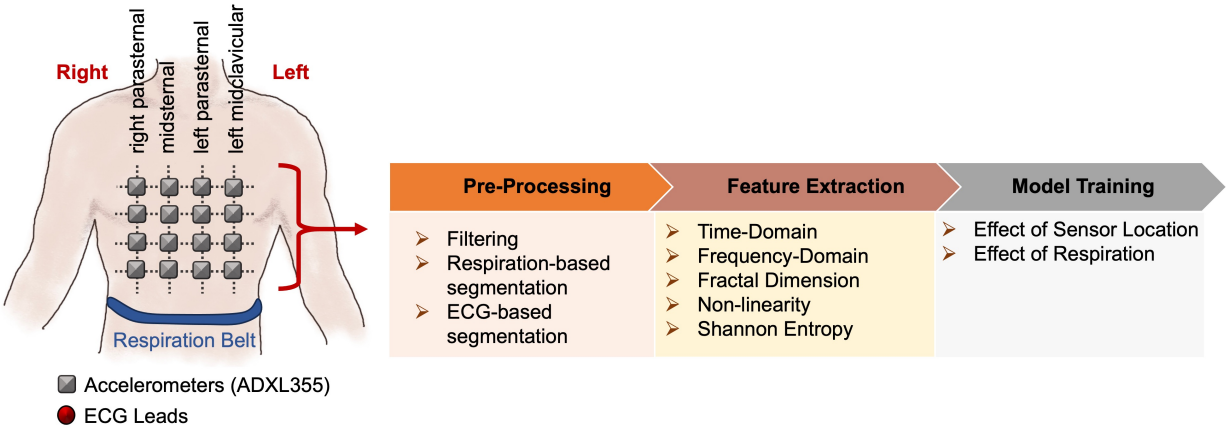


Fig. 1. Sensors in the data collection protocol and the study overview.

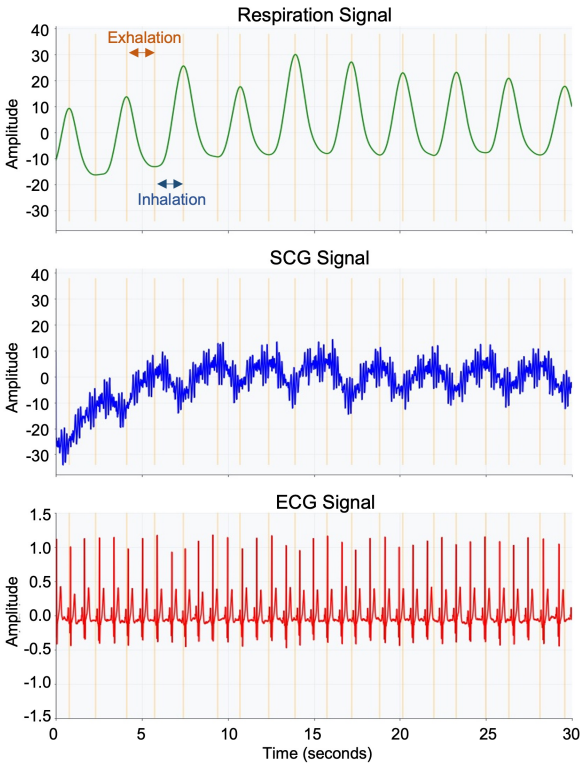


Fig. 2. Sample respiration, SCG and ECG signals from a subject. The signals were divided into inhalation and exhalation segments using the peak and valley locations on the respiration signal.

in indices of Poincaré maps calculated on ECGs and SCGs, which indicates the reliability of SCG as a source signal in non-linear HRV analysis using Poincaré maps [15]. On the other hand, Lyapunov exponents are mathematical quantities used to characterize the sensitivity of a dynamical system to initial conditions. They measure how rapidly nearby trajectories diverge or converge in phase space, providing insights into the long-term behavior and stability of the system. Research indicates that Lyapunov exponents computed from various locations on the body surface exhibit distinct distributions within ECG signals obtained from patients with coronary artery disease and sinus rhythms and from healthy older individuals. Specifically, it is observed that the maximum Lyapunov exponent across all signals manifests as positive, while others display negative values [16]. Considering this observation, Lyapunov exponents associated with SCG signals were also computed.

5) Shannon Entropy: Alterations in the entropy of biosignals have been identified as potential indicators of anomalies or perturbations in physiological dynamics. Specifically, deviations from expected heart rate variability (HRV) entropy patterns have been associated with conditions such as cardiac dysfunction or imbalances within the autonomic nervous system. Thus, Shannon entropy was extracted as the final feature.

D. Model Training and Validation

To assess intra-subject variability on the SCG signals, the effects of sensor location and respiration phases on the SCG signals were investigated. In addition, we analyzed which feature groups and SCG axes (directions) are affected the most by the intra-subject variability introduced by the sensor location and respiration activity. The effects were quantified by treating each scenario as a different classification task. As the classification model, Extreme Gradient Boosting Trees (XGBoost) was utilized. XGBoost belongs to ensemble methods, wherein multiple estimators are employed simultaneously to estimate a variable rather than relying on a single estimator. In the training phase, numerous decision trees are sequentially trained [17]. This process enables the prediction and enhancement of residual errors from the previous iteration over time. For all three tasks, the train and test splits were determined as 80% and 20%, respectively. The parameters were as follows: *eta = 0.1, max_depth = 7, objective = multi:softmax*. The performance of the models were assessed using accuracy, precision and recall metrics.

1) Investigating the Effect of Sensor Location: As shown in Figure 1, there were 16 tri-axial accelerometers attached on the torso. In this scenario, the problem was treated as a 16-class classification task using XGBoost classifier and 80%-20% train-test split. As the features from all three axes for each location were used, there were 30362 beats (24289 for training, 6073 for test) in total.

2) Investigating the Correspondence with the Respiratory System: In the second scenario, it was hypothesized that regardless of the location of the sensors, there will still be visible differences in the morphology of the SCG signal during inhalation and exhalation phases. This is because as the torso expands, the medium characteristics change, hence the vibration patterns (and the SCG morphology) are affected. Therefore, to distinguish between the exhalation- and inhalation-induced beats, the problem was treated as a binary classification task using XGBoost classifier and 80%-20% train-test split. Again, as the features from all three axes for each location were used, there were 30362 beats (24289 for training, 6073 for test) in total.

3) Investigating the Performance of Different Feature Groups: In the final analysis, the tasks performed in previous two scenarios were repeated for (i) different feature groups and (ii) individual accelerometer axes to investigate how different feature groups and SCG axes (directions) are affected by the intra-subject variability introduced by the sensor location and respiration activity. Similar to the previous tasks, XGBoost classifier with 80%-20% train-test split was implemented.

III. Results and Discussion

As explained in Section II-D, we had two main tasks under model training: (i) investigating the effect of sensor location through a 16-class classification model and (ii) investigating whether exhalation and inhalation phases have distinguishable effect on the SCG morphology. In addition, we investigated how these effects translate into individual SCG axis and feature groups. The results for both tasks are presented in the following sub-sections and summarized in Table III-B.

A. Effect of Sensor Location

The 16-class location classification showed that, although we had high number of classes, the XGBoost model achieved an accuracy, recall and precision of %92. In other words, the features extracted from 16 different locations on the chest were distinguishable (i.e. different) from each other with a rate of %92. This effect was visible the most in the dorso-ventral direction (Z-axis) with a rate of %96, followed by lateral (X-axis) and head-to-foot directions (Y-axis) with the rates %92 and %90, respectively.

When individual feature groups were investigated, time domain and frequency domain features achieved a distinction rate up to %85, whereas there was no significant distinction in the remaining feature groups (rates close to random guess). Although this might be due to the presence of relatively lower number of features in remaining individual feature groups, we could only reach up to %27 when we combined all of the remaining features (non-linearity, Shannon entropy and fractal dimension). This shows that the problem was not with the number of features, but due to the fact that the location-based intra-subject variability could not be translated into non-linearity, Shannon entropy and fractal dimension features. On the other hand, having a frequency domain performance of %85 was aligning with our previous work on inter-subject variability. In that work, we showed that the variability in the medium between the accelerometer and heart across different people will result in changing filtering effect on the SCG signals as each person has a unique combination of bone, muscle, fat and skin cells. Apparently, this is also valid for the intra-subject variability as different locations on the chest will have different ratios of bone, muscle, fat and skin cells depending on the organ and system anatomy, affecting the vibration path sensed by the accelerometer.

Effect of Location		**Effect of Respiration**	
	Accuracy		**Accuracy**
ALL FEATURES	0.92	**ALL FEATURES**	0.90
X-axis	0.92	X-axis	**0.95**
Y-axis	0.90	Y-axis	0.90
Z-axis	**0.96**	Z-axis	0.91
Time Domain	0.83	Time Domain	0.84
Frequency Domain	0.85	Frequency Domain	0.82
		Shannon Entropy	0.70

TABLE I
CLASSIFICATION RESULTS FOR THE LOCATION AND RESPIRATION EFFECT

B. Effect of Respiration

In the second task, we investigated the effect of inhalation and exhalation phases on the SCG morphology by treating the problem as a binary classification problem. The XGBoost classifier reached a detection rate of %90 when all features were used. Although we had low number of classes compared to the previous task, the detection performance was worse. This might be because: (i) the effect of respiration phases were relatively subtle compared to sensor location, or (ii) inter-subject variability also had an added-impact on the classification performance.

When the individual axes were investigated, the effect of respiration was more visible in the lateral (X-axis) direction (%95), followed by dorso-ventral (Z-axis) and head-to-foot (Y-axis) directions with distinction rates of %91 and %90, respectively. Under the individual feature groups, time domain and frequency domain features achieved a distinction rate up to %85, time-domain ones having a slightly higher distinction rate. Although remaining features resulted in rates close to random guess, Shannon entropy by itself could achieve a rate of %70. Although it was one single feature, the effect of inhalation and exhalation on its values was significant. As Shannon entropy is associated with potential perturbations in physiological dynamics, it was indeed aligning with the underlying effects of respiration on SCG signals.

IV. Conclusion

In this work, our aim was to investigate how local body compositions and surrounding systems affect the morphology of the SCG signals and extracted features. More specifically, we focused on the effects of sensor location and respiration phases on the SCG signals. Our results revealed that there are distinguishable differences in the features extracted from 16 locations (%92) and the effects of inhalation and exhalation (%90) on the SCG morphology. While the effect of location was more prominent in the dorso-ventral (Z-axis) direction, the phases of respiration showed greater impact in the later (X-axis) direction.

Overall, we showed that the intra-subject variability (caused by sensor location and respiration) has a great impact on the SCG characteristics, therefore should not be ignored during analyses. Especially when the utmost aim is to achieve individualized treatment and remote monitoring, the inaccuracies stemming from intra-subject variability should be minimized to have more generalizable and accurate models. Future work will focus on investigating methods to eliminate the intra-subject variability problem, such as development of calibration algorithms, to be able to achieve more standardized analysis pipelines.

References

[1] O. T. Inan, P.-F. Migeotte, K.-S. Park, M. Etemadi, K. Tavakolian, R. Casanella, J. Zanetti, J. Tank, I. Funtova, G. K. Prisk, *et al.*, "Ballistocardiography and seismocardiography: A review of recent advances," *IEEE journal of biomedical and health informatics*, vol. 19, no. 4, pp. 1414–1427, 2014.

[2] O. T. Inan, M. Baran Pouyan, A. Q. Javaid, S. Dowling, M. Etemadi, A. Dorier, J. A. Heller, A. O. Bicen, S. Roy, T. De Marco, *et al.*, "Novel wearable seismocardiography and machine learning algorithms can assess clinical status of heart failure patients," *Circulation: Heart Failure*, vol. 11, no. 1, p. e004313, 2018.

[3] M. M. H. Shandhi, B. Semiz, S. Hersek, N. Goller, F. Ayazi, and O. T. Inan, "Performance analysis of gyroscope and accelerometer sensors for seismocardiography-based wearable pre-ejection period estimation," *IEEE journal of biomedical and health informatics*, vol. 23, no. 6, pp. 2365–2374, 2019.

[4] B. Semiz, A. M. Carek, J. C. Johnson, S. Ahmad, J. A. Heller, F. G. Vicente, S. Caron, C. W. Hogue, M. Etemadi, and O. T. Inan, "Non-invasive wearable patch utilizing seismocardiography for peri-operative use in surgical patients," *IEEE Journal of Biomedical and Health Informatics*, vol. 25, no. 5, pp. 1572–1582, 2020.

[5] J. Wahlström, I. Skog, P. Händel, F. Khosrow-Khavar, K. Tavakolian, P. K. Stein, and A. Nehorai, "A hidden markov model for seismocardiography," *IEEE Transactions on Biomedical Engineering*, vol. 64, no. 10, pp. 2361–2372, 2017.

[6] M. Imirzalioglu and B. Semiz, "Quantifying respiration effects on cardiac vibrations using teager energy operator and gradient boosted trees," in *2022 44th Annual International Conference of the IEEE Engineering in Medicine & Biology Society (EMBC)*, pp. 1935–1938, IEEE, 2022.

[7] K. Pandia, O. T. Inan, G. T. Kovacs, and L. Giovangrandi, "Extracting respiratory information from seismocardiogram signals acquired on the chest using a miniature accelerometer," *Physiological measurement*, vol. 33, no. 10, p. 1643, 2012.

[8] E. Erin and B. Semiz, "Spectral analysis of cardiogenic vibrations to distinguish between valvular heart diseases.," in *BIOSIGNALS*, pp. 212–219, 2023.

[9] Q. Xu, T. L. Nwe, and C. Guan, "Cluster-based analysis for personalized stress evaluation using physiological signals," *IEEE journal of biomedical and health informatics*, vol. 19, no. 1, pp. 275–281, 2014.

[10] F. Tokmak and B. Semiz, "Investigating the effect of body composition differences on seismocardiogram characteristics," in *2023 IEEE 36th International Symposium on Computer-Based Medical Systems (CBMS)*, pp. 323–328, IEEE, 2023.

[11] K. Munck, K. Sørensen, J. J. Struijk, and S. E. Schmidt, "Multichannel seismocardiography: An imaging modality for investigating heart vibrations," *Physiological Measurement*, vol. 41, no. 11, p. 115001, 2020.

[12] O. O. Nacitarhan and B. Semiz, "Pysio: A new python toolbox for physiological signal visualization and feature analysis," in *2022 44th Annual International Conference of the IEEE Engineering in Medicine & Biology Society (EMBC)*, pp. 3686–3689, IEEE, 2022.

[13] A. Ripoli, A. Belardinelli, G. Palagi, D. Franchi, and R. Bedini, "An effective algorithm for quick fractal analysis of movement biosignals," *Journal of medical engineering & technology*, vol. 23, no. 6, pp. 216–221, 1999.

[14] J. E. Jacob, G. K. Nair, A. Cherian, and T. Iype, "Application of fractal dimension for eeg based diagnosis of encephalopathy," *Analog Integrated Circuits and Signal Processing*, vol. 100, pp. 429–436, 2019.

[15] S. Sieciński, P. Kostka, N. Piaseczna, and M. Wadas, "Comparison of indices derived from poincaré maps on electrocardiograms and seismocardiograms," in *Current Trends in Biomedical Engineering and Bioimages Analysis: Proceedings of the 21st Polish Conference on Biocybernetics and Biomedical Engineering*, pp. 15–24, Springer, 2020.

[16] Z. Wang, Z. Li, Y. Wei, X. Ning, and Y. Lin, "Lyapunov exponents for synchronous 12-lead ecg signals," *Chinese Science Bulletin*, vol. 47, pp. 1845–1848, 2002.

[17] T. G. Dietterich *et al.*, "Ensemble learning," *The handbook of brain theory and neural networks*, vol. 2, no. 1, pp. 110–125, 2002.